ISCI, Volume *15*

Supplemental Information

Unveiling Property of Hydrolysis-Derived DMAPbI$_3$ for Perovskite Devices: Composition Engineering, Defect Mitigation, and Stability Optimization

Yunhe Pei, Yang Liu, Faming Li, Sai Bai, Xian Jian, and Mingzhen Liu

Supplemental Information

This PDF file includes:

Figures S1 to S10

Tables S1 to S3

Transparent Methods

Figures:

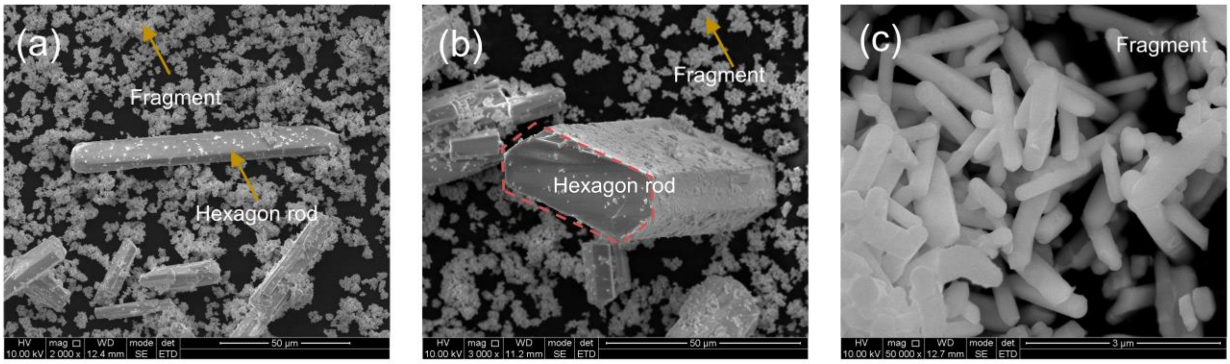

Figure S1. SEM images of lead source powder, Related to Figure 1.

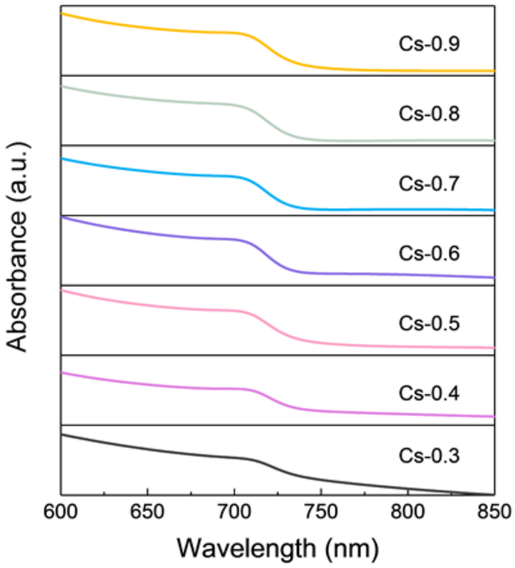

Figure S2. UV-vis spectra of perovskite films, Related to Figure 3.

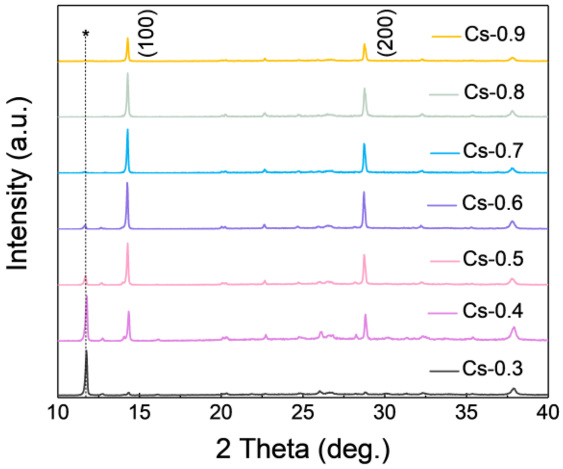

Figure S3. XRD pattern of $Cs_xDMA_{1-x}PbI_3$ perovskites, Peak for $DMAPbI_3$ marked with ‘*’, Related to Figure 3B.

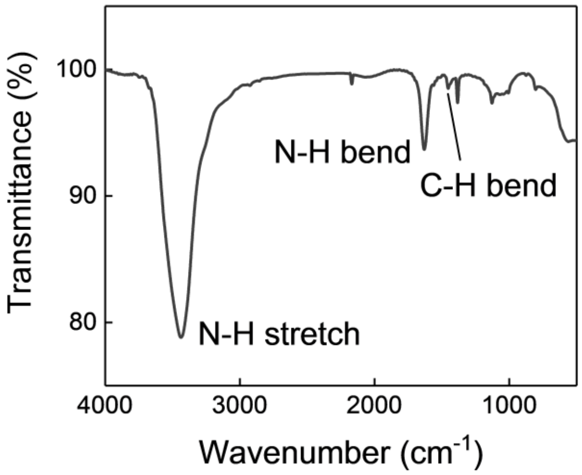

Figure S4. FTIR of powder obtained from scratching away the $Cs_xDMA_{1-x}PbI_3$ film (Cs-0.5), Related to Figure 3.

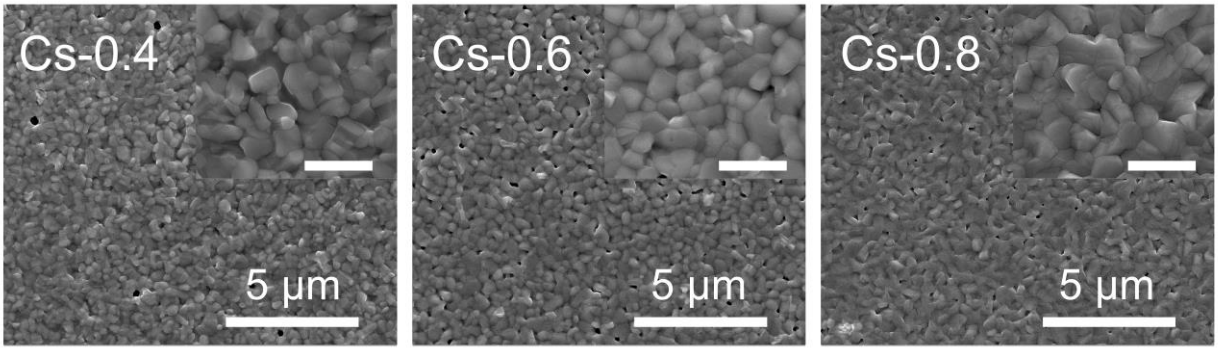

Figure S5. Top view SEM images of perovskite films with different CsI/DMAPbI$_3$ molar ratio, Related to Figure 3D. scale bar is 1 µm in inserted images.

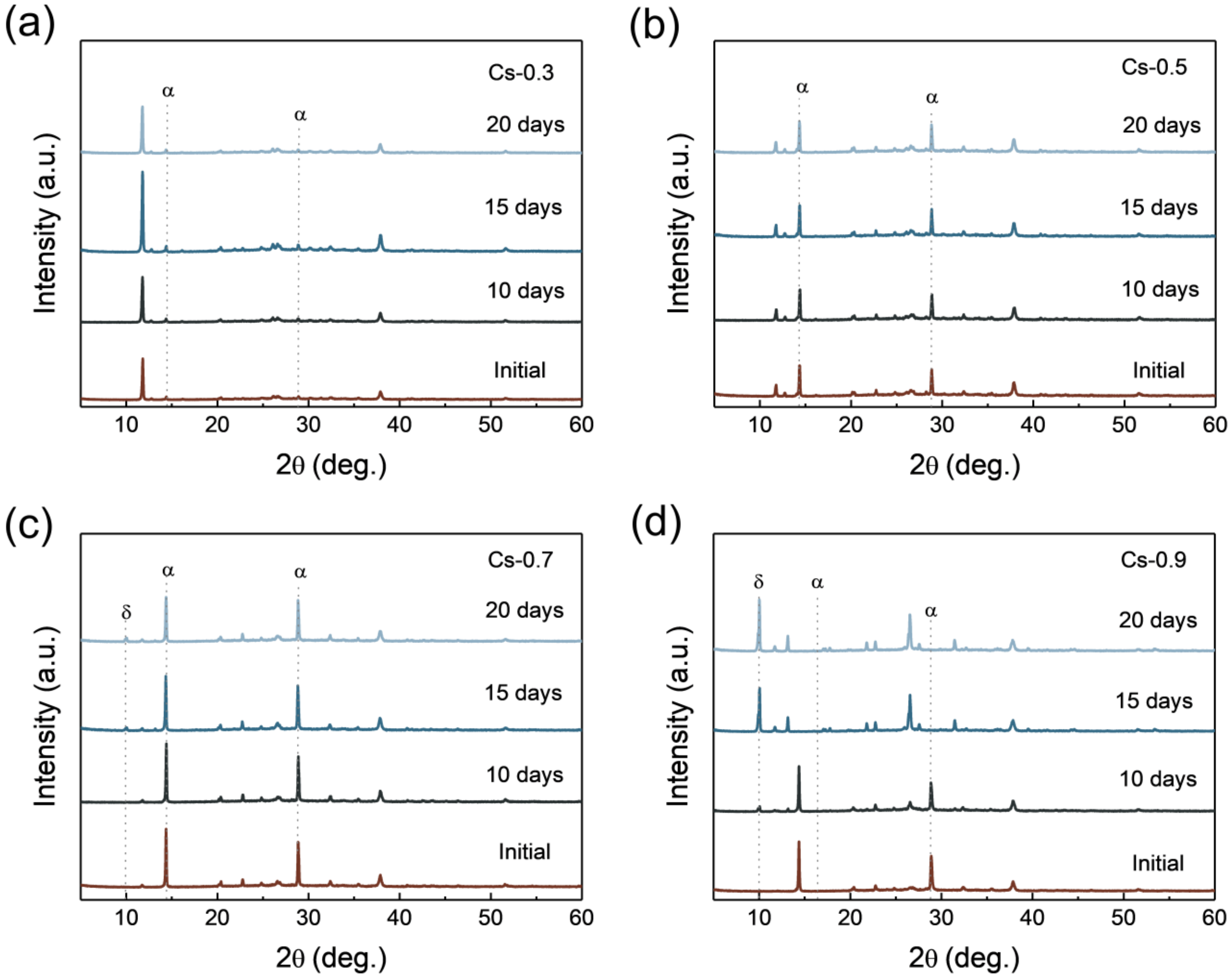

Figure S6. Characterization of perovskite films under humid environment (20±5%). The structural evolution of (a) Cs-0.3 film, (b) Cs-0.5 film, (c) Cs-0.7 film and (d) Cs-0.9 film, Related to Figure 3E.

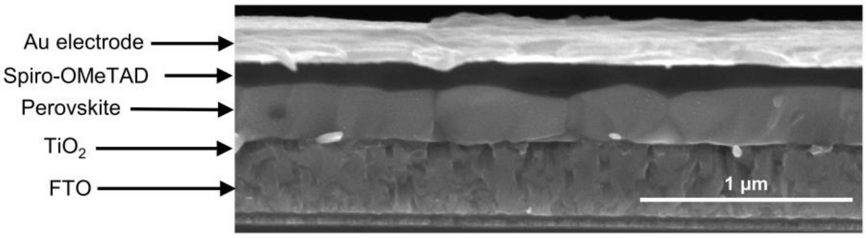

Figure S7. Cross view SEM image of $Cs_xDMA_{1-x}PbI_3$ perovskite solar cells, Related to Figure 5.

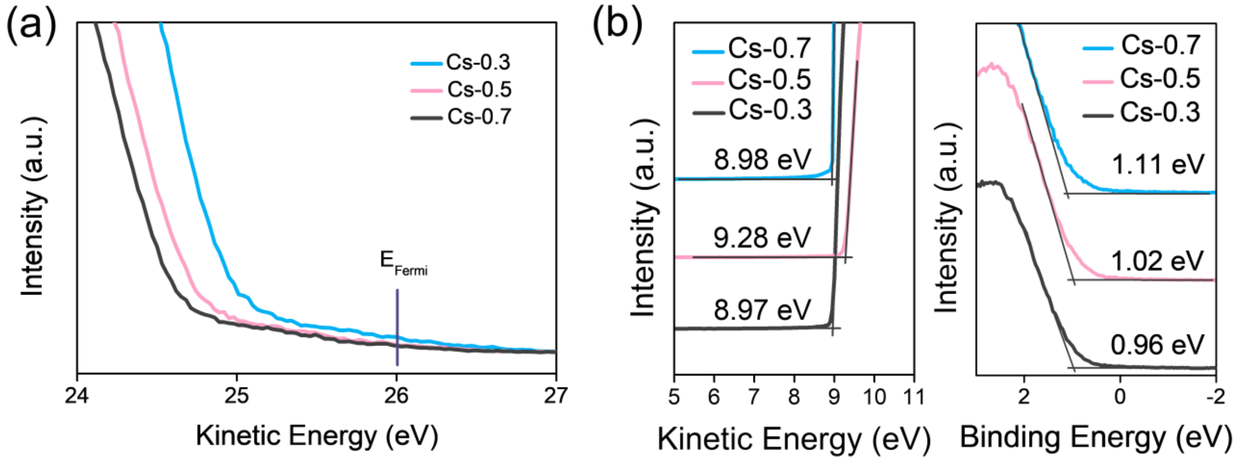

Figure S8. (a) Fermi edge region for perovskite films. (b) UPS cut-off region (left) and VB region (right) of perovskite films. A bias voltage of -5 V was applied. The work function (W_F) can be calculated according to hv-W_F =E_{Fermi} -E_{cutoff}. The W_F can be calculated to 4.17 eV (Cs-0.3), 4.48 eV (Cs-0.5) and 4.18 eV (Cs-0.7), respectively. Related to Figure 5.

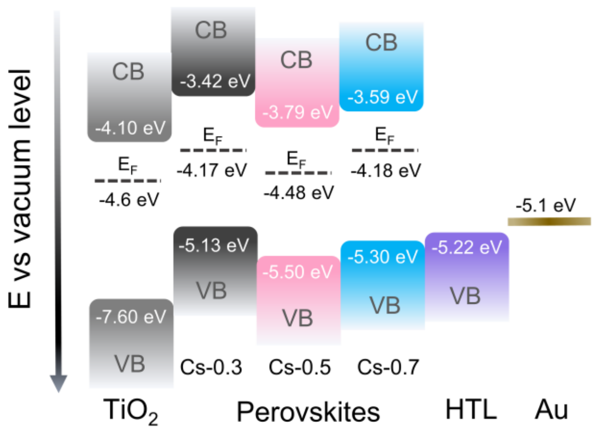

Figure S9. Diagram of energy level of perovskite films, Related to Figure 5.

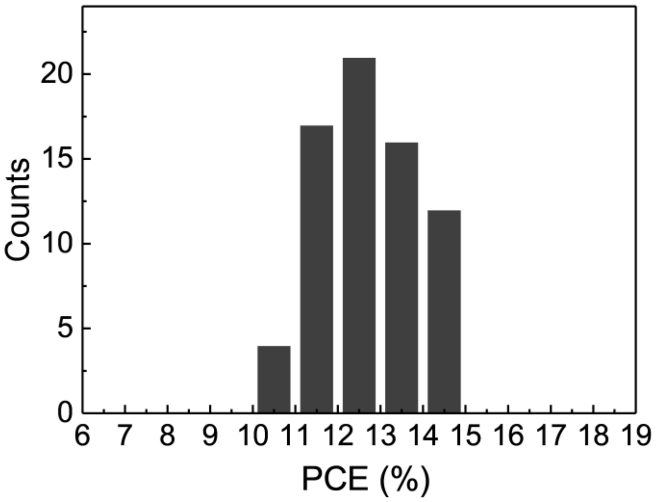

Figure S10. PCE histograms for solar cells based on Cs-0.5 perovskite film, Related to Figure 5.

Tables:

Table S1. Electron trap-state density of $Cs_xDMA_{1-x}PbI_3$ perovskite films, Related to Figure 4 A-D.

$CsI/DMAPbI_3$ molar ratio in precursor	0.3	0.5	0.7	0.9
V_{TFL} (V)	0.30	0.22	0.31	0.41
Trap-state density (cm^{-3})	3.36×10^{15}	3.12×10^{15}	4.32×10^{15}	5.42×10^{15}

Table S2. The fitted PL lifetime of perovskite films, Related to Figure 4F.

Sample	A_1	t_1(ns)	A_2	t_2(ns)	t_{ave} (ns)
Cs-0.3	0.97%	8.2	99.03%	2.1	2.16
Cs-0.5	61.29%	3.5	38.71%	3.5	3.50
Cs-0.7	78.30%	1.8	21.70%	3.4	2.15
Cs-0.9	4.11%	1.5	95.89%	0.6	0.64

Table S3. PV parameters of optimized devices based on various perovskites, Related to Figure 5A.

$CsI/DMAPbI_3$ molar ratio in precursor	0.3	0.4	0.5	0.6	0.7	0.8	0.9
J_{sc} (mA/cm^2)	14.6	17.3	18.4	19.3	19.6	19.5	19.6
V_{oc} (V)	1.009	1.068	1.054	1.019	0.967	0.912	0.899
PCE (%)	9.3	12.9	14.3	13.5	13.1	11.0	10.5
FF	0.63	0.70	0.74	0.69	0.69	0.62	0.60

Transparent Methods

Materials: Hydroiodic acid (HI, Alfa, 57 wt% in H_2O), PbI_2 (99.9%, Sigma-Aldrich), CsI (>99.99%, Xi'an Polymer Light Technology Corp.), lithium bis(trifluoromethanesulfonyl)imide (Li-TFSI, 99.95%, Sigma-Aldrich), 4-tert-butylpyridine (4-tBP, 96%, Sigma-Aldrich), chlorobenzene (Sigma-Aldrich), *N,N*-dimethyiformamide (DMF, 99.8%, Sigma-Aldrich) and all other chemicals were all used as received without further purification. TiO_2 sol (ethanol solution containing a 10% volume fraction of tetrabutyl titanate) was synthesized.

***Preparation of $DMAPbI_3$ powder*:** $DMAPbI_3$ precursor was prepared by dissolving PbI_2 (4.62 g) in DMF (10 mL) and then adding HI (3.6 mL), followed by stirring at 50°C overnight to ensure complete reaction. In order to remove excess HI, the precursor was then washed in absolute ethanol to obtain the light-yellow precipitate. Particularly, the amount of ethanol plays a key role in the synthesis of high quality $DMAPbI_3$ powder. The heating temperature during stirring should be controlled accurately. The obtained powder was dried in vacuum at 65°C for 12 h and stored in a nitrogen glovebox.

***Preparation of $Cs_xDMA_{1-x}PbI_3$ films*:** CsI and $DMAPbI_3$ powder in different molar ratios (CsI from 0.3 M to 0.9 M, $DMAPbI_3$ fixed at 1 M) were dissolved in 1 mL DMF, followed by stirring for 40 min at room temperature (RT). The perovskite films for characterization were formed through spin-coating 70 μL perovskite precursor onto the FTO substrate or the compact TiO_2 substrate at 4000 rpm for 30 s and then annealing at 140 °C for 2 min and 180 °C for 4 min. The transfer of temperature should be finished quickly.

***Device fabrication*:** The device fabrication was conducted based on FTO substrates which were cleaned with deionized water, acetone and ethanol in ultrasonic cleaner. Then FTO substrates were treated in O_2 plasma cleaner for 10 min. For the formation of compact TiO_2 layer, TiO_2 precursor sol was spun-coated on the substrates at 3000 rpm for 30 s, followed by annealing at 500 °C for 30 min in air. The compact TiO_2 coated substrates were then treated with UV-ozone for 10 min. Subsequently, the perovskite layer was deposited via spin-coating. The spiro-OMeTAD precursor was prepared by dissolving 80 mg spiro-OMeTAD with 35 μL LiTFSI solution (520 mg in 1 mL acetonitrile) and 28.8 μl 4-tBP in 1 mL chlorobenzene. Hole transport layer was deposited on top of perovskite film by spin-coating at 4000 rpm for 40 s. Finally, a ~100 nm Au electrode was deposited by thermal evaporation under the pressure of 5×10^{-4} Pa.

***Measurements and Characterization*:** X-ray diffraction (XRD) patterns of films and powder were recorded by a Bruker D8 Advance diffractometer with Cu K_α radiation (λ = 1.5418 Å) and LYNXEYE_XE detector. Scanning electron microscope (SEM) images were collected by FEI Inspect F50 electron microscope with electron energy of 10 keV. The energy disperse spectroscopy analysis (EDS) was also performed on FEI Inspect F50. Steady-state photoluminescence (PL) measurements and time-resolved PL decay were conducted by using FluoTime 300 (PicoQuant). The *J-V* curves were measured by Keithley 2400 series digital source-meter unit and the devices were placed under simulated AM 1.5G irradiation (100 mW/cm^2, xenon lamp, Newport). The effective area of one cell is 0.09 cm^2. Ultraviolet photoelectron spectra (UPS) were carried out by Thermo Fisher Scientific Escalab 250Xi system by using a He discharge lamp (21.22 eV), a bias voltage of -5 V was applied. X-ray photoelectron spectroscopy (XPS) was performed by the same system as UPS. Fourier transform infrared (FTIR) spectra were measured by the Thermo Scientific Nicolet IS 10 FTIR spectrometer. Nuclear magnetic resonance (^{1}H NMR) spectra were measured with Bruker Advance 400 spectrometer. The space-charge-limited current (SCLC) measurements were carried out by Keithley 2400 digital source-meter under dark condition. The external quantum efficiency (EQE) spectra were measured using a QTEST HIFINITY 5 (Crowntech Inc., USA). Thermogravimetry *in situ* infrared spectroscopy (TG-FTIR) coupled analysis was performed on PerkinElmer STA8000 simultaneous thermal analyzer combined with Frontier FTIR. The heating rate is 10 K/min.